Published in final edited form as:
Conf Proc IEEE Eng Med Biol Soc. 2012 ; 2012: 1916–1920. doi:10.1109/EMBC.2012.6346328.

Single Degree-of-Freedom Exoskeleton Mechanism Design for Thumb Rehabilitation*

Yimesker Yihun, **Robert Miklos**, **Alba Perez-Gracia**[1], **David J. Reinkensmeyer**[2], **Keith Denney**, and **Eric T. Wolbrecht**[3]

[1]Dept. of Mechanical Engineering, Idaho State University, Pocatello, ID, USA.

[2]Departments of Mechanical and Aerospace Engineering, Anatomy and Neurobiology, and Biomedical Engineering, University of California, Irvine, Irvine, CA, USA.

[3]Department of Mechanical Engineering, University of Idaho, Moscow, ID, USA.

Abstract

This paper presents the kinematic design of a spatial, 1-degree-of-freedom closed linkage to be used as an exoskeleton for thumb motion. Together with an already-designed finger mechanism, it forms a robotic device for hand therapy. The goal for the exoskeleton is to generate the desired grasping and pinching path of the thumb with one degree of freedom, rather than using a system actuating all its joints independently. In addition to the path of the thumb, additional constraints are added in order to control the position and size of the exoskeleton, reducing physical and sensory interference with the user.

I. Introduction

Robotic devices have been shown to be capable of automating the strenuous and repetitive nature of movement therapy after stroke or other neurological injury (for an introduction, see [1], [2]). Additionally, robotic devices give scientists a new investigative tool for recording progress during movement training and for determining the factors that promote functional recovery. Of particular interest is the ability to design, implement, and test assistive control strategies. Many different control strategies have been developed (see review: [3]). The most promising approaches fall into the assist-as-needed category, where an attempt is made to vary the level of assistance to match the impairment level of the patient. For example, [4] presents an assist-as-needed controller that learns a model of the patients abilities while simultaneously reducing assistance when the patient performs well. The result is a robotic device that can help patients complete movements but continuously challenges them to try. The efficacy of these and other control strategies has been documented ([5], [6], [7]) but it remains unclear what specific controller characteristics increase patient learning during therapy.

Proper evaluation of assist-as-needed control strategies is dependent upon the abilities of the robotic device. Ideally, the device would be able to apply any force at any speed at any location along the movement trajectory. In practice, this is impossible, but can be approached in a robotic device by keeping apparent inertia and friction low, and the

*This work was partially supported by Grant Number NIHR01HD062744-01 from NCHHD, and by the US Department of the Army, award number W81XWH-10-1-0128 awarded and administered by the U.S. Army Medical Research Acquisition Activity. The content is solely the responsibility of the authors.

yihuyime@isu.edu, miklrobe@isu.edu, perealba@isu.edu dreinken@uci.edu kmdenney@gmail.com, ewolbrec@uidaho.edu

controllable force bandwidth high. To achieve these features, we are developing an exoskeleton device for the fingers and thumb, with the actuators mounted along the forearm where their effect on device inertia is minimized. In addition, the actuators are high-speed, low-friction linear motors, which allows for high-bandwidth control. These characteristics have not been fully achieved in previous robotic hand and wrist devices, including end-effector, glove, and exoskeleton type devices ([8], [9], [10]).

The device presented in this paper is obtained following a new methodology for the design of exoskeletons. Traditionally, exoskeletons are designed so that they try to align with the human joint axes of motion [8]. This assumes that the location of the axis can be accurately known, and in addition, that such a fixed axis exists for the range of motion of the joint or set of joints, which is not always the case. A clear example of complex kinematic modeling is the thumb, for which precise detection methods such as MRI segmentation [11] show that considering fixed rotational axes, especially for the CMC joint, is not a good approximation; see also [12]. Using the methodology described in this paper, based on kinematic synthesis, it is not necessary to know the geometry of the hand, but rather to have a description of its motion at the point of attachment.

To meet the design needs for the rehabilitation application described above, a lightweight single-degree-of freedom mechanism has been selected for following the paths of the thumb during simple pinch and grasping movements. The complete exoskeleton device consists of two separate single degree-of-freedom exoskeleton mechanisms: one for finger curling motions, whose design was presented in [13], and one for thumb motions, presented in this paper. The resulting robot will be able to assist in common, naturalistic finger and thumb motions. As such, the therapy delivered should translate to a wide range of functional tasks, even if the degrees-of-freedom of the robot are minimal.

The linkage to perform the thumb motion was selected among several single-degree-of-freedom spatial closed linkages with four to six links, with a single end-effector for controlling the orientation and position of the proximal phalanx of the thumb. In this approach, the mechanism will be actuated with a single actuator, and so the design of the mechanism is responsible for appropriately shaping the thumb motion. In addition, the designed mechanism is confined to the back of the hand, so as to minimize sensory feedback interference, and to allow the mechanism to be manufactured with minimal size. This combined with the intended location of the actuators will allow the device to be constructed with low apparent inertia.

II. Thumb Mechanism Design

A. Design objectives

The human thumb presents a complex 3D motion that can be modeled, depending on the needed accuracy, with three to four degrees of freedom, and using variable joint axes. For this project, the targeted task of the thumb is a single spatial path going from index pinching to contacting the tip of the fingers. We postulate that it is still possible to use simplified, low-dof linkages for assisting in this motion. We focus on a set of closed, spatial overconstrained and non-overconstrained four-bar to six-bar linkages with low mobility that present the desired characteristics for this application, see [14] and [15]. The spatial mechanism is to be attached to the proximal phalanx of the thumb. The goal is to find a single-dof mechanism whose path is as close to the experimental thumb path as possible, while complying with additional size and placement constraints.

B. Thumb data

The method is based on synthesize a linkage to follow as closely as possible experimental paths of the human thumb. The thumb data was acquired using a Vicon motion tracking system. The set up we used had eight infrared cameras set around the room, primarily for larger applications; however it worked very well for the hand motions. The markers that are used with the system are small white balls that reflect the inferred light. We used arrays with the markers placed 1.25 inches apart making it easy to collect data in the three dimensions. In order to assess the exact location of the fixed link with respect to the hand, additional sets of sensors are placed on the arm, see Figure 1

The several experimental paths so obtained were separated for clarity; Figure 2 shows one typical point path, seen from the reference frame of the motion capture system.

For the design of spatial motion, it is sometimes advantageous to work with relative displacements. Each relative displacement expresses a motion of the thumb from a reference configuration, taken as the thumb position at the first frame. Each displacement can be modeled as an axis, plus a rotation about and a translation along the axis. We encode this information as a *screw*, where the screw axis is the axis of the displacement and the pitch is the ratio of translation to rotation for that displacement.

Figure 3 shows the displacements of the thumb's proximal phalanx path as screw axes with a pitch, where the screw lengths are proportional to the pitch. The screw axes of the displacements with their pitches generate a *screw hyper-surface*. This representation has all the information of the motion except for the value of the rotation, which can be calculated independently.

C. Mechanism Selection

In order to accomplish simplicity together with spatial motion under a one-degree-of-freedom system, an initial set of closed spatial linkages with four to six links and standard revolute (R), prismatic (P) and cylindrical (C) joints has been selected. Some of these linkages are overconstrained, while others are trivial linkages, all of them with mobility equal to one [14], [15]. Figure 4 shows the topology of the spatial CCCC linkage (a linkage with four cylindrical joints); candidate linkages with four links are particular cases of this one, obtained by making some of the joint variables (θ_i, r_i) constant.

Similarly, the closed, spatial CCC-CCC linkage can be seen as the general case for the six-bar candidate linkages, see Figure 5. In particular, the following four-bar linkages: RC-CC, RP-RP, RR-RR, and the following six-bar linkage: CRR-RRR were selected as candidates. Here, the dash separating joints indicates where the end-effector, or attachment to the thumb, is being placed.

In order to asses the suitable topology for the thumb linkage, the workspace of relative displacements has been analyzed for each of these linkages. Figure 6 shows a typical workspace for the candidate linkage.

From inspection of the workspace shape, the candidate linkages to be used for dimensional synthesis are the RRRR, the RC-CC and the CRR-RRR. The RRRR is an overconstrained linkage, while the other two present trivial mobility equal to one.

Among the properties of these linkages that are useful for our application we can cite the 1-dof motion, requiring only one actuator, and topological simplicity while creating a complex motion. In addition, overconstrained linkages have other advantages, such as inherent structural rigidity.

D. Mechanism Design Equations

In this section, the design equations corresponding to the CRR-RRR mechanism are presented. The reason to do so is that it turned out to give the most fitted mechanisms for the task.

Let us consider the closed CRR-RRR linkage as two serial chains, CRR and RRR, joined at their end-effectors. The axes are labeled as shown in Figure 5, starting at the fixed C joint and going around up to the final fixed R joint. For every joint *i*, let $\mathsf{s}_i = \mathbf{s}_i + \in \mathbf{s}_i^o$ be the joint axis, with rotation θ_i, and slide (for the C joint only) d_i. We express the forward kinematics equations of the CRR and RRR chains using dual quaternions [16],

$$\begin{aligned} \widehat{Q}_{CRR}\left(\Delta\widehat{\theta}_1, \Delta\theta_2, \Delta\theta_3\right) &= \prod_{i=1}^{3}\left(\cos\tfrac{\Delta\widehat{\theta}_i}{2} + \sin\tfrac{\Delta\widehat{\theta}_i}{2}\mathsf{S}_i\right) \\ \widehat{Q}_{RRR}\left(\Delta\theta_6, \Delta\theta_5, \Delta\theta_4\right) &= \prod_{i\in\{6,5,4\}}\left(\cos\tfrac{\widehat{\Delta}\theta_i}{2} + \sin\tfrac{\widehat{\Delta}\theta_i}{2}\mathsf{S}_i\right) \end{aligned} \quad (1)$$

where $\Delta\widehat{\theta}_i = \Delta\theta_i + \in \Delta d_i$ is the dual angle, and all $d_i = 0$ except d_1 corresponding to the cylindrical joint. The forward kinematics so expressed represent the set of relative displacements of the chain with respect to a reference configuration.

In order to create the design equations, we minimize the distance between the displacements captured in Section II.B. and the displacements of the candidate chain. We perform dimensional synthesis, that is, the goal is to find the location and dimensions of the mechanism that performs approximately the task.

The design equations are created by equating the forward kinematics of the mechanism to each of the discrete positions obtained from the motion capture. If we denote each finite displacement of the thumb as $\widehat{P}^i$, we can create the relative displacements with respect to the first position of the thumb, $\widehat{P}^{1i} = \widehat{P}^i\left(\widehat{P}^1\right)^{-1}$, to yield design equations

$$\begin{aligned} &\widehat{Q}_{CRR}\left(\Delta\widehat{\theta}_1^i, \Delta\theta_2^i, \Delta\theta_3^i\right) = \widehat{P}^{1i}, \\ &\widehat{Q}_{RRR}\left(\Delta\theta_6^i, \Delta\theta_5^i, \Delta\theta_4^i\right) = \widehat{P}^{1i}, \qquad i = 2, \ldots, m. \end{aligned} \quad (2)$$

In these equations, the variables we are interested in are what we call the *structural variables*, which are the Plucker coordinates of the joint axes $\mathsf{s}_i = \mathbf{s}_i + \in \mathbf{s}_i^o$ at the reference configuration. In addition, the optimization process outputs the angles of the chains in order to reach the thumb displacements.

To complete the system of equations in (2), we impose size constraints on the mechanism so that it can be attached to the lower arm and with reasonable dimensions. In particular, for the six-link CRR-RRR mechanism, we add the constraints of distance between both fixed axes and also between the fixed axes and the thumb,

$$\begin{aligned} \mathsf{S}_1 \cdot \mathsf{S}_6 &= \cos\alpha + \in a\sin\alpha \\ \mathsf{S}_1 \cdot \mathsf{P}^1 &= \cos\beta + \in b\sin\beta \end{aligned} \quad (3)$$

where P^1 is the screw axis of the first thumb position, and we fix the distance between the axes along the common normal, *a*, to a value between 50mm and 150mm, and the distance between the thumb attachment and the coupler axes, *b*, to similar values.

E. Implementation of the Design Equations

Ten positions were selected from the thumb path, and the first frame was taken as the reference configuration. Each forward kinematics equality is composed of 8 equations, and forward kinematics are written for both serial chains composing the mechanism. This gives a total of 144 nonlinear equations. In addition, we have the constraints of (3). Overall, we have 147 equations.

The variables to solve for are the Plucker coordinates of the axes, that is, six parameters per axis, and the joint variables to reach each thumb position. The total is 97 unknowns.

The equations were solved using a Levenberg-Marquardt nonlinear, unconstrained solver implemented in Java. This is based on public domain MINPACK routines, translated from FORTRAN to Java by Steve Verrill [17].

III. Results

The best results were obtained for the CRR-RRR mechanism. One of the sets of ten equally-spaced positions selected from the thumb data can be seen in Figure 9. The equations were run 14 times for three different sets of positions chosen from the thumb frames. The distance to the desired path has been optimized by minimizing the distance at each step. The overall error of the function was smaller than 0.03, and it took a variable amount of time, from a few minutes to a few hours, to find solutions. For these 14 runs, 14 considerably different solutions were found.

Out of these 14 solutions, 2 linkages were selected because of their overall dimensions and placement on the hand. Figure 7 shows the SolidWorks model of those solutions, named candidate I and II.

As overall solution, we selected the mechanism with the best combination of fit to the path, dimensions and placement. Due to the potentially very large number of solutions for this problem, not all the solution space has been searched and hence we cannot assume that the selected candidate is the optimal one, but rather an acceptable one.

Figures 8 and 9 present the actual motion of the linkage as compared to the thumb path and design poses. Even though there is some small divergence in the paths, we must point out that it is of the order of the variability of the several paths observed in the motion capture data, rendering an overall motion that is within the normal thumb actuation.

Rapid prototypes have been built in order to assess the manufacturing and to better design the hand attachment and compatibility with the finger exoskeleton. Figure 10 shows one of the prototype linkages mounted on the hand.

IV. Conclusions and Future Work

This paper presents a task-oriented design methodology for exoskeletons. Previous work targeted planar motion, while this paper focuses on the application to spatial motion. In particular, we apply the methodology to develop a 1-dof thumb exoskeleton for rehabilitation. The kinematic design is followed by a detailed mechanical design and prototyping.

The main advantage of this method with respect to previous exoskeleton designs is that it does not need any assumption about location and type of joints in the subject; the exoskeleton is going to follow the path that is selected as task regardless of the skeleton structure that generates it. This allows for the creation of new and innovative exoskeleton

designs. The high number of solutions obtained mean more choices for the designer regarding placement, size, and inertia of the exoskeleton.

The final designs presented in this paper have been tested for the desired path and the results seem to be acceptable. The placement of the mechanism on the lower arm and close to the wrist is also according to specifications.

The next step is the force analysis of the mechanism. This is important because of the spatiality of the linkage, and will allow us to determine the best joint to place the actuator.

Future research for the mechanism optimization includes identifying a small subset of structural variables that, when modified, will produce a new mechanism to track a similar path created by a slightly different thumb. In a fashion similar to [18], this will allow the mechanism to be re-configured to varying subject sizes.

References

[1]. Frick EM, Alberts JL. Combined use of repetitive task practice and an assistive robotic device in a patient with subacute stroke. Physical Therapy. 2006; vol. 86(10):1378–1386. [PubMed: 17012642]

[2]. Reinkensmeyer, DJ.; Galvez, JA.; Marchal, L.; Wolbrecht, ET.; Bobrow, JE. Some key problems for robot-assisted movement therapy research: A perspective from the university of california at irvine. In: ASME. , editor. Proc. 10th IEEE Intl. Conf. on Rehabilitation Robotics; Noordwijk, The Netherlands. 2007. p. 1009-1015.

[3]. Crespo LM, Reinkensmeyer DJ. Review of control strategies for robotic movement training after neurologic injury. J Neur Eng Reh. 2008 vol. submitted.

[4]. Wolbrecht ET, Reinkensmeyer DJ, Bobrow JE. Optimizing compliant, model-based robotic assistance to promote neurorehabilitation. IEEE Transactions Neural Systems and Rehabiltation Engineering. 2008; vol. 16:286–297.

[5]. Brewer BR, McDowell SK, Worthen-Chaudhari LC. Post-stroke upper extremity rehabilitation: a review of robotic systems and clinical results. Top. Stroke Rehabil. 2007; vol. 14:22–44. [PubMed: 18174114]

[6]. Krebs HI, Mernoff S, Fasoli SE, Hughes R, Stein J, Hogan N. A comparison of functional and impairment-based robotic training in severe to moderate chronic stroke: a pilot study. NeuroRehabilitation. 2008; vol. 23:81–87. [PubMed: 18356591]

[7]. Mehrholz J, Platz T, Kugler J, Pohl M. Electromechanical and robot-assisted arm training for improving arm function and activities of daily living after stroke. Cochrane Database Syst. Rev. 2008; vol. 4:CD006876. [PubMed: 18843735]

[8]. Balasubramanian S, Klein J, Burdet E. Robot-assisted rehabilitation of hand function. Curr. Opin. Neurol. 2010; vol. 23(6):661–670. [PubMed: 20852421]

[9]. Itoa S, Kawasakia H, Ishigureb Y, Natsumec M, Mouria T, Nishimotod Y. A design of fine motion assist equipment for disabled hand in robotic rehabilitation system. J. Franklin Inst. 2009 vol. doi:10.1016/j.jfranklin.2009.02.009.

[10]. Worsnopp, T.; Peshkin, M.; Colgate, J.; Kamper, D. An actuated finger exoskeleton for hand rehabilitation following stroke. Proc. 10th IEEE Intl. Conf. on Rehabilitation Robotics; The Netherlands. Noordwijk; 2007. p. 896-901.

[11]. Stillfried, G.; van der Smagt, P. Movement model of a human hand based on magnetic resonance imaging (mri). Proceedings of the 1st Int. Conf. on Applied Bionics and Biomechanics; Venice, Italy. October 14-16,, 2010;

[12]. Chalon, M.; Grebenstein, M.; Wimbock, T.; Hirzinger, G. The thumb: Guidelines for a robotic design. Proc. of the 2010 Int. Conf. on Intelligent Robots and Systems; Taipei, Taiwan. October 18-22, 2010;

[13]. Wolbrecht, E.; Reinkensmeyer, D.; Perez-Gracia, A. Single degree-of-freedom exoskeleton mechanism design for finger rehabilitation. Proceedings of the ICORR 2011: Int. Conference on Rehabilitation Robotics; Zurich, Switzerland. June 29-July 1, 2011; 2011.

[14]. Waldron K. A study of overconstrained linkage geometry by solution of closure equations - part ii- four-bar linkages with lower pair joints other than screw joints. Mechanism and Machine Theory. 1973; vol. 8:233–247.

[15]. Tsai, L-W. Enumeration of Kinematic Structures According to Function. CRC Press; 2000.

[16]. Perez Gracia, A.; McCarthy, JM. The kinematic synthesis of spatial serial chains using clifford algebra exponentials. Proceedings of the Institution of Mechanical Engineers, Part C, Journal of Mechanical Engineering Science; 2006. p. 953-968.

[17]. Verrill, S. Optimization java package. 2000. http://www1.fpl.fs.fed.us/optimization.htmlhttp://www1.fpl.fs.fed.us/optimization.html[Online]. Available:

[18]. Sands, D.; Perez-Gracia, A.; McCormack, J.; Wolbrecht, E. Design method for a reconfigurable mechanisms for finger rehabilitation. Proceedings of the 2010 IASTED Robotics and ApplicationsConference; Cambridge, Massachusetts, USA. November 1 3, 2010; 2010.

Fig. 1.
Markers placed in the thumb and data capture setup

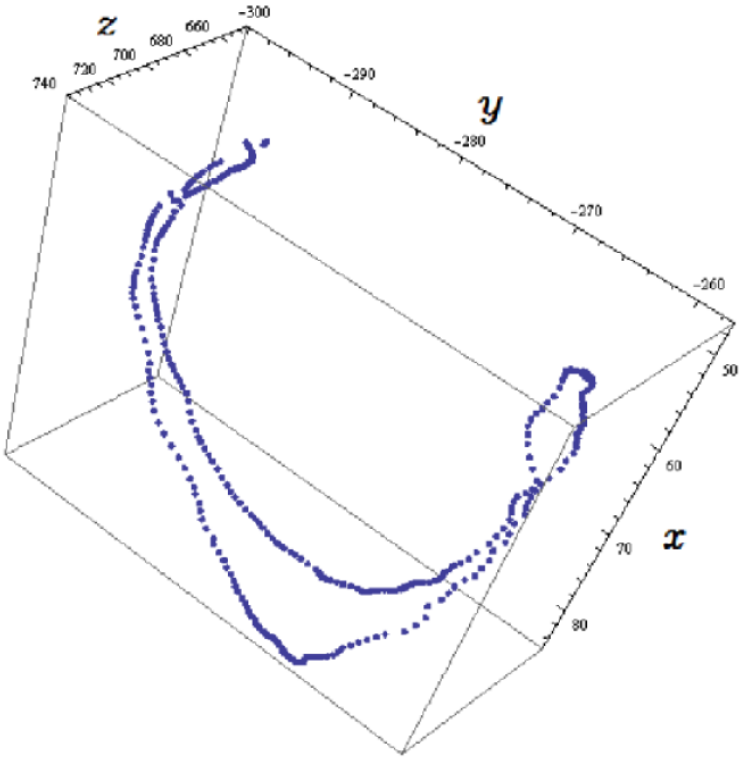

Fig. 2.
Thumb's proximal phalanx point path

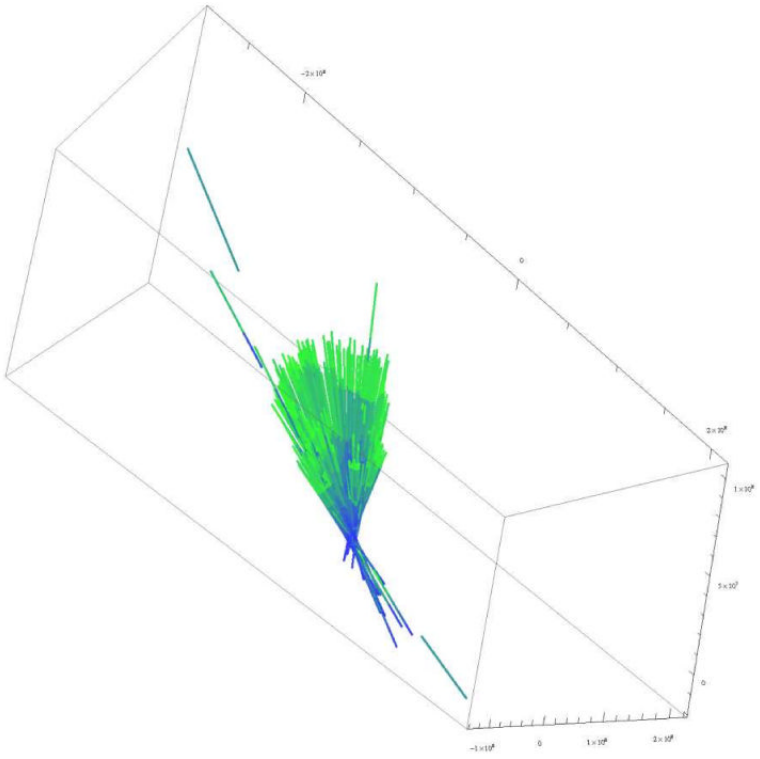

Fig. 3.
Thumb’s proximal phalanx path: screw surface of relative screw axes

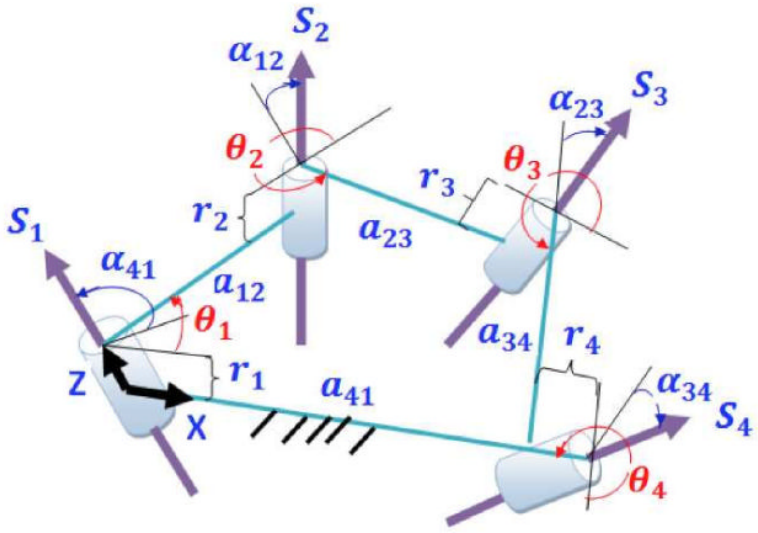

Fig. 4.
A spatial 4-bar CCCC linkage

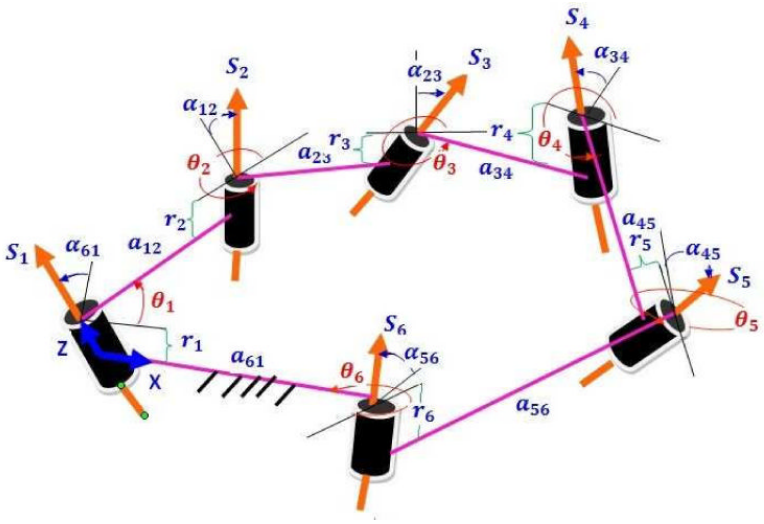

Fig. 5.
A spatial 6-bar CCCCCC linkage

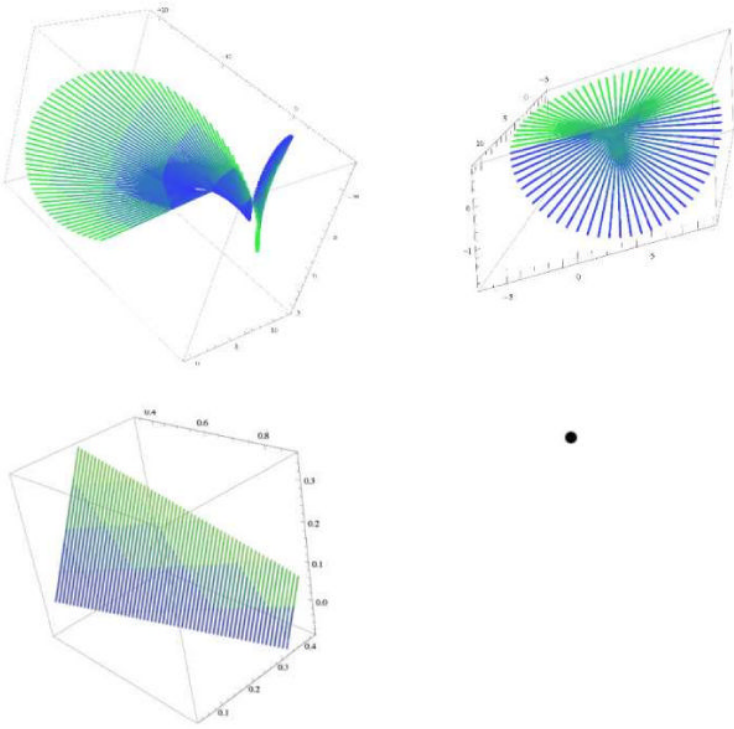

Fig. 6.
Workspaces of the CCCR, the RRRR, the RPRP linkages

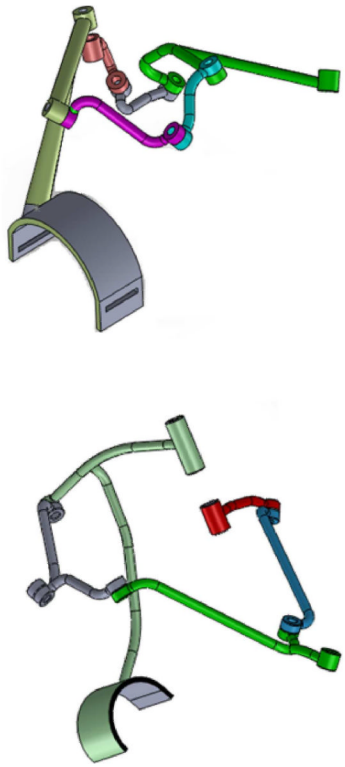

Fig. 7.
The two solutions selected for prototyping

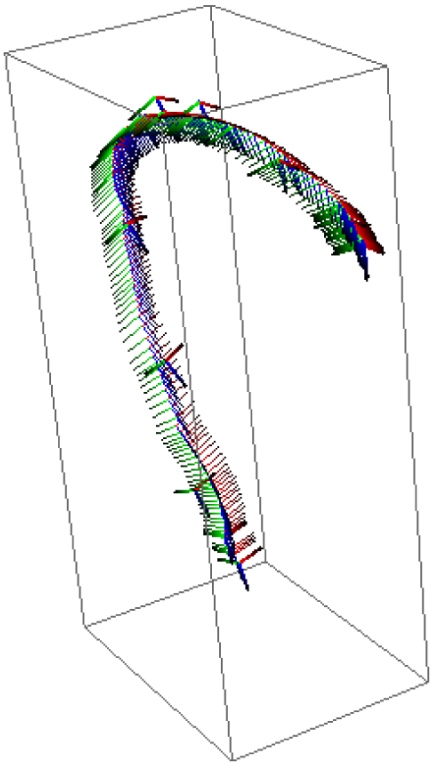

Fig. 8.
One of the thumb paths (thin frames) with superimposed linkage path (thick lines)

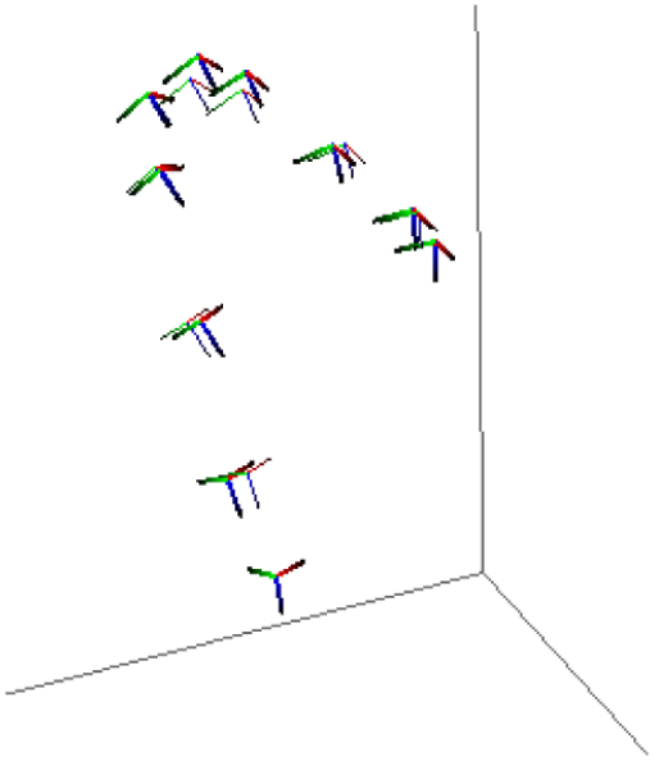

Fig. 9.
Comparison between design positions (thin lines) and linkage positions (thick lines)

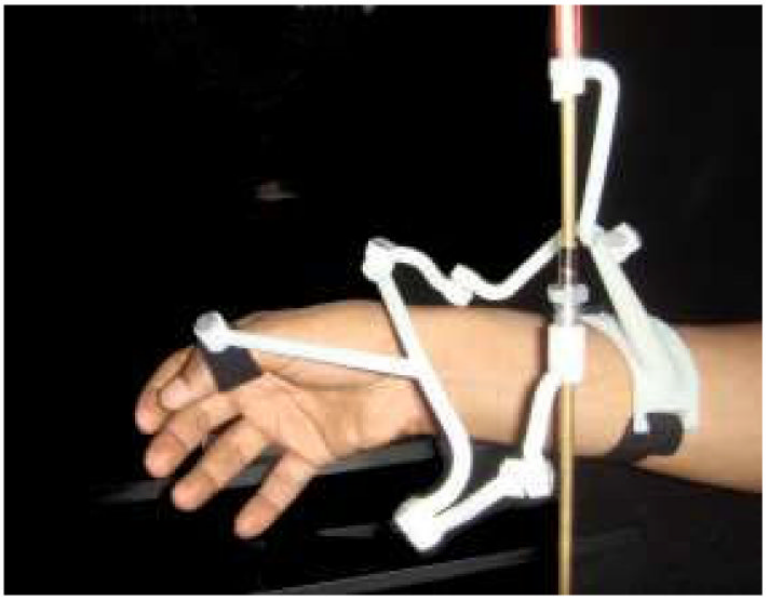

Fig. 10.
One prototype attached to the thumb